Journal Title: Journal of wind engineering and industrial aerodynamics.

Volume: 89
Issue: 14-15
Month/Year: December 2001
Pages: 1219-1232

Article Author: M. Kiya, , a, H. Ishikawab and H. Sakamotoc;

Article Title: Near-wake instabilities and vortex structures of three-dimensional bluff bodies; a review

Imprint: [Amsterdam] ; Elsevier Scientific Pub. Co.,

ELSEVIER

Journal of Wind Engineering
and Industrial Aerodynamics 89 (2001) 1219–1232

JOURNAL OF wind engineering AND industrial aerodynamics

www.elsevier.com/locate/jweia

Near-wake instabilities and vortex structures of three-dimensional bluff bodies: a review

M. Kiya[a,*], H. Ishikawa[b], H. Sakamoto[c]

[a] *Kushiro National College of Technology, Nishi 2 Otanoshike, Kushiro 084-0916, Japan*
[b] *Division of Mechanical Science, Graduate School of Engineering, Hokkaido University, N13W8, Kita-ku, Sapporo 060-8628, Japan*
[c] *Department of Mechanical Engineering, Kitami Institute of Technology, 165 Koencho Kitami 090-8507, Japan*

Abstract

Instabilities and vortical structure in the near wake of a sphere and a circular disk are reviewed, together with those of an elliptic disk and rectangular plate which have two length scales. The linear global instability analysis (J. Fluid Mech. 254 (1993) 323) yields critical Reynolds numbers of regular and Hopf bifurcations of the sphere wake, which are in excellent agreement with direct numerical simulations and experiments. The Strouhal number of shedding of hairpin-like vortices in the sphere wake is significantly dependent on Reynolds number, reflecting changes in the wake such as transition from laminar to turbulent wakes. The vortex structure at high Reynolds numbers still remains to be clarified. Two periodic components of velocity fluctuations are found in the wake of elliptic disks and rectangular plates, being likely to be caused by global instability in the near wake.

Keywords: Wakes; Instabilities; Bluff body wakes; Low-frequency unsteadiness; Vortex shedding; Vortex structure

1. Introduction

In wind engineering, flows around an axisymmetric body such as a sphere or a circular disk are less encountered than those around cylindrical bodies such as a circular or rectangular cylinder. The wake of a sphere is a prototypical wake of

*Corresponding author. Tel.: +81-154-57-8410; fax: +81-154-57-5360.
E-mail address: kiya@office.kushiro-ct.ac.jp (M. Kiya).

0167-6105/01/$ - see front matter
PII: S0167-6105(01)00160-X

axisymmetric bodies but is not as well understood as its two-dimensional counterpart, the wake of a circular cylinder. Studies to date indicate that vortex structure in the wake of the sphere is substantially different from that in the wake of the circular cylinder, and thus little of what has been learned for wakes of two-dimensional bluff bodies is directly applicable to symmetric wakes. In his review on bluff-body aerodynamics, Roshko [2] mentioned that nominally axisymmetric flows deserve more attention from laboratory and numerical experiments in relation to possible extraneous effects from end conditions in nominally two-dimensional flows.

The wakes of an elliptic plate and a rectangular plate, which are normal to the main flow, are much less studied than the wake of the sphere, although they are associated with flow around side-view mirrors of cars, non-axisymmetric parachutes, airships during cross winds, and many others. These bodies have two length scales and two planes of symmetry, thus being expected to have wake structures different from those of a sphere or a circular disk. The wakes of the plane-symmetric bluff bodies with low aspect ratio also serve to study transition of vortical structures from cylindrical bodies to axisymmetric bodies. It should also be noted that the wake of a square plate normal to the flow is not understood yet.

In this review we are concerned with vortical structure in the wake of the axisymmetric and plane-symmetric bluff bodies at rest in a steady uniform flow. The lock-on phenomena and active control of vortex shedding from a sphere are also reviewed.

2. Instabilities and vortex structure in sphere wake

2.1. Instabilities

Flow around a sphere in a uniform main flow separates from the surface to form a steady toroidal vortex at Reynolds number R of 20, where R is defined in terms of the main-flow velocity U and the diameter of the sphere d. The steady flow changes to an asymmetric steady flow through a normal bifurcation at $R = R_{c1} = 210$. This value of R_{c1} was obtained by Natarajan and Acrivos [1] who employed a global linear stability analysis by assuming the velocity perturbations in the form of $\sum_m v^{(m)}(r, z) \exp(\sigma_m t + \mathrm{i}m\theta)$, where m is the mode number, (r, z, θ) is the cylindrical coordinate system with the axis aligned with the main flow, t is time, σ_m is the complex growth rate, and $v^{(m)}(r, z)$ is a function of r and z. The most unstable mode is $m = 1$, which is a helical mode. This steady flow changes to a new unstable flow of mode $m = 1$ through a Hopf bifurcation at $R = R_{c2} = 277.5$; the fundamental frequency f_2 is $S_2 (= f_2 d/U) = 0.113$ in the form of Strouhal number.

For a circular disk Natarajan and Acrivos [1] obtained the values of $R_{c1} = 116$, $R_{c2} = 125.6$ and $S_2 = 0.126$. At both Reynolds numbers R_{c1} and R_{c2}, the eigenfunctions for the sphere and the circular disk have striking similarity, indicating that these two unstable modes have the same physical origin in the two bodies.

The values of the critical Reynolds numbers and the Strouhal number for the sphere are confirmed by direct numerical simulations (DNS) and experiments. The

Tomboulides et al.'s [3] DNS yielded $R_{c1} = 212$, $R_{c2} = 250$–285, and $S_2 = 0.116$. The growth rate of the $m = 1$ mode is in excellent agreement with the linear stability analysis in the range of $R = 160$–300. Ormieres and Provansal [4] experimentally obtained the amplitude of the longitudinal velocity fluctuation in the wake as a function of Reynolds number to show, by extrapolation, that the amplitude becomes zero at $R_{c2} = 280 \pm 6$. Flow visualization experiments show that $R_{c2} = 270$ [5,6] and $R_{c2} = 280$ [7]. Sakamoto and Haniu [8] obtained a higher value of $R_{c2} = 300$ by hot-wire measurements. This is probably because the growth rate of the unstable $m = 1$ mode is too low to be detected by the hot-wire probes at Reynolds numbers close to R_{c2}.

2.2. *Vortex structures near-critical Reynolds numbers*

The vortex structure in the wake of the sphere changes in the following way through the critical Reynolds numbers. In the range of $R_{c1} < R < R_{c2}$ the flow is characterized by a double-thread vortical structure which comprises two parallel vortex tubes extending downstream from the end of the recirculation zone [4,9–11]. The double thread has a planar symmetry. The transition at $R = R_{c1}$ is argued to be associated with an azimuthal instability of the low-pressure core of the toroidal vortex [10].

The double thread is conjectured to be the stable solution for supercritical values of R and its spatial form can be obtained from the eigenfunction of the unstable mode. The full theoretical justification of this conjecture requires a nonlinear analysis of the stability of the entire class of bifurcating solutions, which consists of arbitrary linear combinations of the unstable mode superposed with different azimuthal phases [1]. It is worth noting that a superposition of the $m = 0$ and 1 modes yields a fork-like vortical structure in the sphere wake, depending on the local amplitude of the $m = 1$ mode; the fork approaches the sphere as Reynolds number increases [12].

In the range of $R > R_{c2}$, hairpin-shape vortices with one-sided orientation are periodically shed from the sphere (Fig. 1). Numerical simulations show that the hairpin vortices have planar symmetry up to $R = R_{c3} = 350$–375 [3,13]. The orientation of the hairpin vortices and thus the plane of symmetry are conjectured to be determined by small irregularities in the main flow and initial conditions. This conjecture is supported by the fact that, when a sphere is placed in a uniform shear flow, the top of the hairpin vortices is fixed at the high-speed side of the shear flow [14]. The formation of the hairpin vortices is completed $(4.5$–$5.5)d$ downstream of the center of the sphere at $R = 280$–360 since the energy of velocity fluctuation attains a maximum at this position as shown by Ormieres and Provansal [4].

The DNS of Johnson and Patel [10] in the range $R = 270$–300 shows not only one-sided hairpin vortices, but also previously unrevealed, oppositely oriented hairpin vortices, which are conjectured to be induced by the interaction of the near-wake flow and the outer flow. This seems to be due to the nature of their flow visualization, the oppositely oriented hairpin vortices being much weaker than the other.

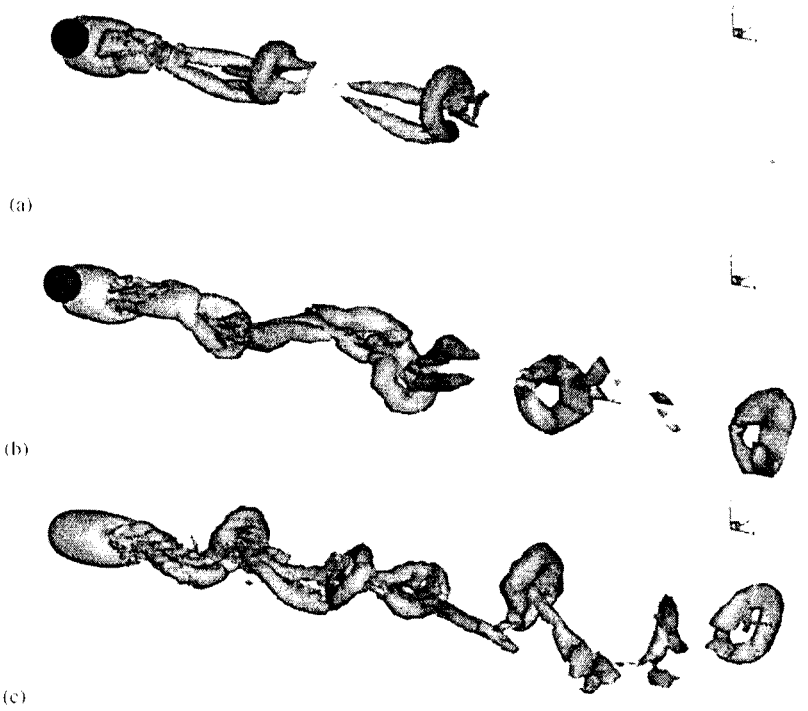

Fig. 1. Vortical structure in the sphere wake at (a) $R = 350$, (b) $R = 500$ and (c) $R = 650$ [16].

The fixed orientation of the hairpin vortices yields the time-mean and fluctuating lift force in the particular direction [10,13]. The frequency of the fluctuating lift is the same as the vortex-shedding frequency. The r.m.s. value of the fluctuating lift is of the order of 1/10th of the time-mean drag, being much lower than that of the fluctuating lift of a circular cylinder which is of the same order as the time-mean drag. This suggests that the circulation of the hairpin vortices is much lower than that of Karman vortices in the wake of the circular cylinder.

2.3. *Vortex structures in the range of* $R > R_{c3}$

The orientation of hairpin vortices tends to change from cycle to cycle at $R > R_{c3}$, thus the planar symmetry is lost. The cycle-to-cycle change becomes more and more irregular as Reynolds number increases [3,15,16]. The power spectrum of velocity fluctuation at $R = 500$ [3] shows a peak at a frequency f_L on top of a primary peak which corresponds to the vortex shedding f_v, f_L being of the order of $(1/3 - 1/4)f_v$. The low-frequency component is interpreted as the central frequency of the irregular rotation of the hairpin vortices. At this Reynolds number the hairpin vortices are still laminar although they are fairly distorted by the slow rotation. This is supported by

the fact that the power spectrum has low level of high-frequency components which corresponds to turbulence. The low-frequency component is also observed in the DNS of Mittal and Najjar [16]. Moreover, vortex rings are formed in the downstream region of the wake at $R = 500$ and 650 [5,16].

The large-scale structure at $R = 1.0 \times 10^3$ is similar to that at $R = 500$; lower frequencies of the same order as at $R = 500$ are also observed. A power-spectrum peak appears at a higher frequency than at the vortex-shedding frequency f_v, being interpreted as the frequency of Kelvin–Helmholtz instability of the separated shear layer f_{KH}. The existence of vortices associated with this instability is confirmed by experiments [8,17]. Small-scale vortices, associated with the shear-layer instability, cause a rapid distortion of the large-scale structures and eventually the wake becomes turbulent.

A large-eddy simulation (LES) was made at $R = 2.0 \times 10^4$ by Tomboulides et al. [3]. The hairpin vortices are not identifiable owing to random, small-scale structures. The time history of drag has a high-frequency component corresponding to the shear-layer instability on top of the vortex-shedding component f_v. This seems to be reasonable because vortex rings with significant circumferential coherence is shown to be generated by the shear layer instability [18]. A DNS at the same Reynolds number was performed by Kuwahara [19] in an early stage of the impulsively started flow. The shear-layer instability and the small-scale vortices are observed but the large-scale structure is not clear. A proper data processing is needed to study the nature of large-scale structures in the sphere wake at Reynolds numbers of the order of 10^3–10^4. It may be noted that no numerical simulations have been made at $R > 2.0 \times 10^4$.

The vortex structure at higher Reynolds numbers than 2.0×10^4 is experimentally studied by flow visualizations and hot-wire measurements. Achenbach [20] employed four hot-wire probes near the surface arranged in the circumferential direction with the same distance to show that there exists a structure rotating in the circumferential direction in the range of $R = 6.0 \times 10^3$–3.0×10^4. This structure can be interpreted as the irregular rotation of the separation line azimuthally around the rear part of the sphere. Taneda's flow-visualization [21] experiments at $R = 2.3 \times 10^4$ show a progressive wave motion with a planar symmetry; the plane of symmetry rotates slowly and irregularly around the axis of the wake. This wave motion, which is observed in the range of $R = 1.0 \times 10^4$–3.5×10^5, suggests the shedding of hairpin vortices from the sphere, but it is not clear whether they are one-sided or oppositely oriented.

No helical structures are observed in Taneda's experiment [21]. On the other hand, Berger et al. [18] found, by measurements of coherence of pressure fluctuations at two points in the near wake, that the helical mode $m = 1$ is dominant at $R < 10^5$, while the modes $m = 1$ and 0 are observed approximately at the same probability in the range of $R = 10^5$–2.0×10^5. The flow around the sphere in this range of Reynolds number is sensitive to the residual turbulence and other irregularities in the main flow since the drag crisis occurs approximately at $R = 2.0 \times 10^5$. Thus, the vortical structure in the wake is possibly sensitive to these effects. More detailed studies are needed to resolve this issue.

In a higher range of $R = 3.8 \times 10^5$–1.0×10^6 the separation from the surface is not symmetric in the circumferential direction but such that an attached hairpin vortex is formed whose legs extend downstream to form a pair of streamwise vortices. The vortex pair is shifted in the direction normal to the main flow by the mutual interaction. The vortex pair is fairly steady with no periodic vortex shedding, although it rotates slowly and randomly about the axis. There is no information on large-scale vortex structures at Reynolds numbers higher than 10^6.

2.4. *Vortex-shedding frequency*

The vortex-shedding frequency f_v and the frequency of the shear-layer instability f_{KH} are functions of Reynolds number [8,17,20]. Strouhal numbers defined by $S_v = f_v d/U$ and $S_{KH} = f_{KH} d/U$ are plotted against R in Figs. 2 and 3 [8]. The vortex-shedding frequency is experimentally observed at R higher than approximately 300. The reason why this value is greater than the critical Reynolds number R_{c2} has been explained before. The value of S at this Reynolds number is 0.14, being almost the same as that obtained by DNS [3].

The Strouhal number of vortex shedding S_v are sensitive to Reynolds number as seen from Fig. 2. The relation between the Strouhal number S_v and the vortex structure in the wake is as follows according to Sakamoto and Haniu [8].

(1) $300 < R < 420$: The one-sided hairpin vortices are shed periodically. The velocity fluctuation in the wake is sinusoidal with fairly constant amplitude. The upper limit of this range $R = 420$ is not far from the critical Reynolds number

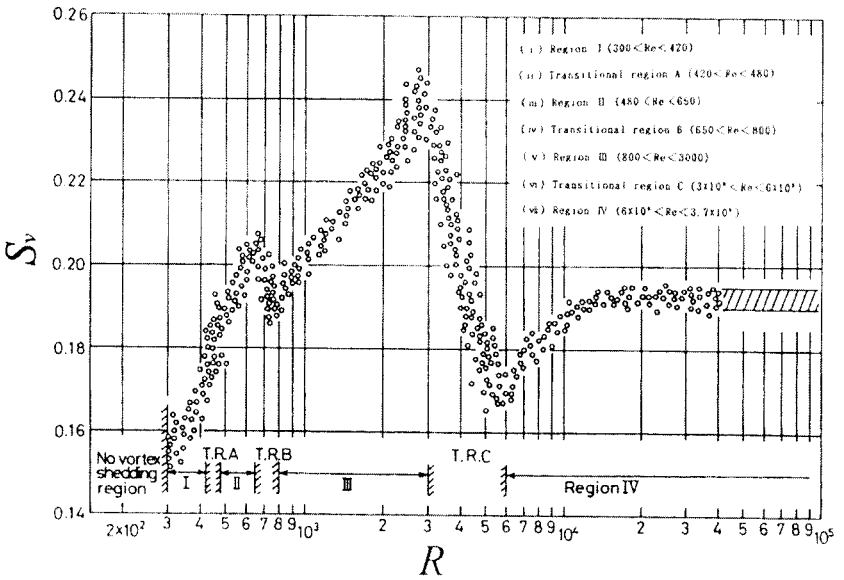

Fig. 2. Strouhal number of vortex shedding S_v versus Reynolds number R for sphere [8].

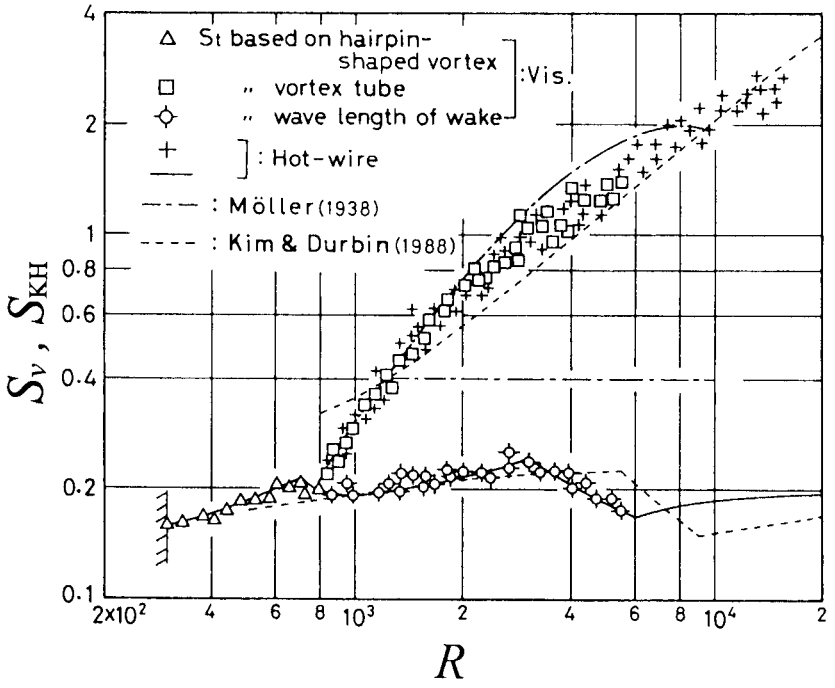

Fig. 3. Strouhal number of shear-layer instability S_{KH} (upper branch) and that of vortex shedding S_v (lower branch) versus Reynolds number R for sphere [8].

$R_{c3} \simeq 350$–375 beyond which the planar symmetry of the hairpin vortices is no longer preserved. The Strouhal number increases with increasing R.

(2) $420 < R < 480$: This is the transition region between regime (1) and regime (3) which will be described below. The angle of the hairpin vortices is constant during a time interval while it changes from cycle to cycle during a following time interval. This process is repeated irregularly. The velocity fluctuation in the wake is sinusoidal in the former while the amplitude is irregularly modified in the latter.

(3) $480 < R < 650$: The angle of hairpin vortices changes irregularly from cycle to cycle to yield the velocity fluctuation in the wake which is basically sinusoidal but the amplitude is irregularly modified. The flow in the wake is laminar. The Strouhal number increases with increasing R.

(4) $650 < R < 800$: The hairpin vortices experience transition from laminar to turbulent flow. Details of the transition are not yet clarified. The Strouhal number decreases with increasing R.

(5) $800 < R < 3.0 \times 10^3$: The separated shear layer starts to develop the Kelvin–Helmholtz instability at $R = 800$. The shear layer is still laminar although the hairpin vortices are turbulent as also confirmed by DNS of Tomboulides et al. [3] at $R = 1.0 \times 10^3$. The Strouhal number increases again with increasing R.

(6) $3.0 \times 10^3 < R < 6.0 \times 10^3$: The rolling-up vortices in the separated shear layer experience transition from laminar to turbulent flow. The position of transition

approaches the separation point with increasing Reynolds number. The Strouhal number decreases from 0.24 to 0.17 with increasing R. This is because the enhanced diffusion of vorticity by the transition requires longer time to accumulate a sufficient amount of circulation in the vortex-formation region with increasing Reynolds number.

(7) $6.0 \times 10^3 < R < 3.7 \times 10^5$: The separated shear layer is turbulent from the separation point, and the hairpin vortices are turbulent [3,19]. The power spectrum of velocity fluctuations in the wake has a definite peak at the vortex-shedding frequency, which can be distinguished from turbulence components [8]. In the range of $R = 6.0 \times 10^3$–2.0×10^5 the boundary layer at separation is expected to be laminar, so that the momentum thickness of the separated shear layer near the separation point decreases with increasing R in the same range. This decrease in the momentum thickness causes the increase in the vortex-shedding frequency. The vortex-shedding frequency is fairly constant at $R > 2.0 \times 10^5$ because the boundary layer is already turbulent at the separation point.

(8) $R > 3.7 \times 10^5$: As mentioned before, an attached hairpin vortex is formed whose legs extend downstream to form a pair of streamwise vortices. This vortex pair is fairly steady with no periodic vortex shedding.

2.5. *Frequency of shear-layer instability*

The shear-layer instability is observed in the range of $R = 800$–6.0×10^4 [8,17], as shown in Fig. 3. The critical value $R = 800$ is lower than the corresponding value for a circular cylinder, that is, $R = 1.2 \times 10^3$ for parallel vortex streets and $R = 2.6 \times 10^3$ for oblique vortex streets [22]. The frequency of the shear-layer instability of a circular cylinder is related to Reynolds number in the form $f_{KH}/f_v = 0.0235R^{0.67}$ for R up to 10^5. This relation can be written as $f_{KH}/f_v = (R/262)^{0.67}$. Prasad and Williamson [22] argue that some sort of resonance is caused at $R \approx 260$ by an interaction between the wake and the shear layer, when f_{KH}/f_v would be equal to unity, although the shear-layer instability is not manifested for $R < 1.2 \times 10^3$ for hot-wire measurements. This argument is supported by the fact that the Karman vortex shedding is particularly spanwise coherent at $R \approx 260$. In addition, the velocity fluctuations appear to be particularly periodic at the same Reynolds number, producing a distinctly sharp peak at f_v in long-time averaged velocity spectra.

In the case of a sphere the shear-layer instability begins to be observed at $R \approx 800$, at which its frequency f_{KH} is equal to the vortex-shedding frequency f_v. No information is available to suggest that a similar resonance as for the circular cylinder is also the case for the sphere at this Reynolds number. This is probably because the shear-layer instability is of mode $m = 0$ while the vortex shedding is of mode $m = 1$. The frequency of the shear-layer instability can be approximated by $f_{KH}/f_v = 0.0113R^{0.75}$, on the basis of Sakamoto & Haniu's experimental results [8]. The ratio f_{KH}/f_v is influenced by the variation of base pressure, frequency of vortex shedding and upstream motion of the transition point, as Reynolds number is increased.

On top of the two frequencies f_v and f_{KH}, there exists the low-frequency modulation whose typical frequency is of the order of $(1/3 - 1/4)f_v$, as mentioned before. This low-frequency modulation was discovered by DNS at $R = 350$–1.0×10^4 [3,16]. The modulation is expected to exist at higher Reynolds numbers but no measurements have been made of the typical frequency of the modulation.

3. Wake of a circular disk

For a circular disk normal to the main flow, Natarajan and Acrivos [1] obtained by the linear stability analysis the critical Reynolds numbers $R_{c1} = 116.5$ and $R_{c2} = 126.5$, and the fundamental frequency $S_2 = 0.126$. The most unstable mode is helical $m = 1$. The value of R_{c1} has not been confirmed either experimentally or numerically. A flow-visualization experiment for a cone of included angle of 90° [6] shows that the wake becomes unsteady at $R = 140$, which is not far from the value of R_{c2}. More experiments are needed to confirm the predicted critical Reynolds numbers and the fundamental frequency. No DNS has been performed for the flow around a circular disk.

Experiments on the wake of a circular disk were performed at Reynolds numbers of the order of 10^3–10^5 [18,23,24]. In this range of Reynolds number, Strouhal number of vortex shedding is fairly constant $S_v = 0.13$–0.15. The main results of the experiments may be summarized in what follows:

(1) An antisymmetric highly coherent structure is observed, which is dominated by helical modes $m = 1$ and -1 at a natural frequency $S_v = 0.135$, at which the helical structures rotate around the axis of the wake [18,23]. The helical structure develops from location of the maximum pressure fluctuation, which occurs just upstream of the rear stagnation point of the recirculating zone, rather than from the edge of the disk. This suggests that the origin of the helical structure is associated with instability of flow in the recirculating zone.

It is timely here to mention a linear stability analysis of Monkewitz [25] on an axisymmetric wake. A family of axisymmetric velocity profiles is employed which allows for the variation of the wake depth as well as for a variable ratio of wake width to the shear-layer thickness. The analysis shows that the first helical mode $m = 1$ is absolutely unstable in the near wake for Reynolds numbers (based on the wake diameter and the main-flow velocity) in excess of 3.3×10^3. This suggests that the large-scale helical vortex shedding, which is observed for the circular disk, may be driven by a self-excited oscillation in the near wake. The frequencies in the absolutely unstable region is in fairly good agreement with experiments. The same is also true for spheres in the range between Reynolds numbers 6.0×10^3 and 3.7×10^5 although no helical structures are observed in the sphere wake.

In the flow visualization of Miau et al. [24] at $R = 1.0 \times 10^3$ hairpin vortices are shed from the disk; the angle of shedding changes irregularly from cycle to cycle. This is similar to the case of the sphere wake. The anti-phase characteristics of vortex

shedding are generally preserved in the near wake at the circumferential positions 180° apart at $R = 2.8 \times 10^4$–8.4×10^4. The anti-symmetric characteristics, however, are unable to distinguish between hairpin vortices and helical structures.

(2) The shear-layer instability yields ring vortices in the immediate wake. These vortices tend to incline and link together, so that the $m = 0$ mode is not distinct as expected for ring vortices. The frequency of the shear-layer instability is not yet obtained as a function of Reynolds number.

(3) Berger et al. [18] observed an axisymmetric pumping of the recirculation zone without formation of ring vortices, which is dominated by an $m = 0$ mode at a low frequency of 0.05 in the form of Strouhal number. The pumping motion is interpreted as enlargement and shrinkage of the recirculating zone. The frequency is of the order of $(1/3)f_v$, being approximately equal to the frequency of the low-frequency modulation for the sphere, which is interpreted as the frequency of the irregular rotation of the hairpin vortices.

(4) Finally, it may be noted that helical structures are dominant in the wake of the circular disk while no evidence for helical structures has been obtained in the sphere wake. This is interesting because the linear stability analysis of Natarajan and Acrivos [1] strongly suggests that the unstable modes have the same physical origin in the two bodies. More detailed studies are needed to clarify the intrinsic similarity and difference between the two wakes. Moreover, although vortex structures in the sphere wake are clarified by DNS and flow-visualization experiments at Reynolds numbers less than 1.0×10^3, no such studies have been made for the wake of the circular disk.

4. Wakes of elliptic and rectangular plates

4.1. Vortex structure and vortex shedding

An elliptic plate normal to the main flow, which has two length scales, is expected to have wake properties between axisymmetric and two-dimensional bluff bodies. Kuo and Baldwin [26] discovered an unexpected result that the far wake of elliptic plates with aspect ratio AR of 1.67 and 5.0 have elliptical cross sections, but the major axis of the wake is aligned with the minor axis of the body; the aspect ratio is defined by $AR = L/D$, where L is the major diameter and D is the minor diameter. This effect was observed in both time-mean velocity and turbulence intensity in the wake throughout the range of the experiment, from several minor diameters to distances of 250 diameters downstream of the body. They also found a periodic velocity fluctuation in the major plane on top of that in the minor plane. More detailed studies on the elliptic wakes have been performed by Kiya and Abe [27], disclosing several novel aspects of the elliptic wakes.

Michalski et al. [28] measured the periodic vortex shedding in the wake of a circular cylinder with free hemispherical ends to study the transition from the cylinder wake to the sphere wake, at Reynolds number R (based on the main-flow velocity U and D) < 375. The critical Reynolds number at which the vortex shedding

occurs is a function of aspect ratio AR, which is defined as the length of the cylinder divided by the cylinder diameter D. The frequency of vortex shedding f_v in the form of Roshko number $R_o = f_v D^2/\nu$ ($= S_v R, \nu$: kinematic viscosity) generally increases with increasing R. This frequency was measured only in the mid span of the cylinder, so that they did not present the second periodic component which is expected to exist in the major plane, as in the case of elliptic and rectangular plates [26,27].

In what follows, the vortex structure and the vortex shedding in the wake of elliptic plates with the aspect ratio of AR = 2.0 and 3.0 will be discussed on the basis of Kiya and Abe [27]. Reynolds numbers based on U and D are $R = 200$ and 2.0×10^4. It may be noted that the wake of rectangular plates has basically the same property as that of the elliptic plates of the same aspect ratio.

The flow visualization and DNS at $R = 200$ showed that hairpin vortices are alternately shed in the minor plane (Fig. 4). The hairpin vortices are oppositely oriented like Karman vortices for cylindrical bodies, and their top is basically in the minor plane of the body. No helical structures are observed.

Velocity contours in the wake in the cross sections normal to the main flow are approximately elliptic up to approximately (4.0–4.5)D downstream of the elliptic plates of aspect ratios of 2.0 and 3.0, the major and minor axes of the wake being aligned with those of the body, respectively. Beyond this position the velocity contours are also approximately elliptic but the major axis of the wake is aligned with the minor axis of the body and vice versa. This phenomenon is referred to as the axis switching in view of the similar phenomenon found in a jet issuing from an elliptic nozzle [29,30].

The mechanism of the axis switching in the wake is completely different from that in the jet. In the elliptic jet the axis switching is caused by the self-induced deformation of elliptic vortex loops shed from the nozzle and the merging interaction between neighbouring vortex loops, as demonstrated by Hussain and Husain [30]. In the elliptic wake, however, no elliptic vortex loops are generated along the edge of the elliptic plate; rather, the hairpin vortices are generated near the end of recirculating zone. The axis switching occurs because the hairpin vortices move outwards by the self-induced velocity, increasing the width of the wake in the minor plane. On the other hand, the width of the wake in the major plane decreases due to the in-flow accompanied by the out-flow in the minor plane, by the requirement of

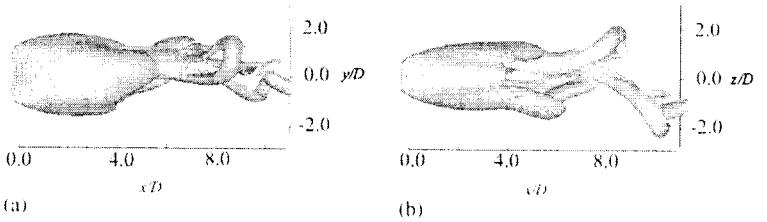

Fig. 4. Eqi-vorticity surface in (a) major plane and (b) minor plane for elliptic plate of aspect ratio AR = 2.0 at $R = 200$ [27].

continuity, over several minor diameters downstream. The crossover of the widths occurs around (4.0–4.5)D downstream of the body, which is the position of the axis switching.

The alternate shedding of the hairpin vortices generates periodic velocity fluctuations in the minor plane, as first found by Kuo and Baldwin [26]. The vortex-shedding frequency f_{vm} is a function of the aspect ratio of the body as shown in Fig. 5, in which f_{vm} is normalized in the form of Strouhal number $S_{vm} = f_{vm}D/U$. Kiya and Abe [27] confirmed the existence of another periodic velocity fluctuation in the major plane, which is also mentioned by Kuo and Baldwin [26]. This frequency f_{vM} is also a function of AR, and is included in Fig. 5 in the form of Strouhal number $S_{vM} = f_{vM}D/U$.

A vortical structure which is responsible for the periodic component in the major plane has not been revealed yet. Both the flow visualizations and DNS at Reynolds number of $R = 200$ suggest that this periodic component is caused by a meandering motion of the hairpin vortices in the direction of the major axis. The frequency in the major plane f_{vM} is a smooth function of the aspect ratio, so that this frequency is expected to be associated with the intrinsic instability in the near wake. It is not established, however, whether the meandering motion is also the case at much higher Reynolds numbers such as $R = 2.0 \times 10^4$.

The frequencies of the periodic components plotted against the aspect ratio are almost the same for the elliptic plate and the rectangular plate at the same Reynolds number. The axis switching is also the case for the two bodies. These facts strongly suggest that the vortex structure in the wake is basically the same for the two bodies, despite the existence of sharp corners in the rectangular plate. The periodic components should be attributed to the global instability of the near wake, whose analysis has not been attempted yet. Such an analysis is challenging because unstable modes should be three-dimensional, having two fundamental frequencies and different growth rates near the major and minor planes. It might be possible that the axis switching can be interpreted by the difference in the growth rates.

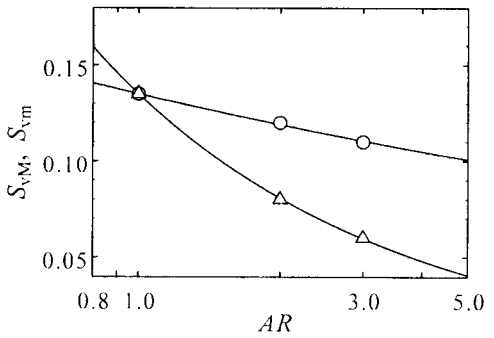

Fig. 5. Strouhal number S_{vm} (circles) and S_{vM} (triangles) for elliptic plate versus aspect ratio AR at $R = 2.0 \times 10^4$ [27].

4.2. Low-frequency modulation

A low-frequency modulation is observed for the vortex shedding in the minor plane and the meandering motion in the major plane [27]. The representative frequency of modulation of the vortex shedding is approximately 1/5 of the vortex-shedding frequency f_{vm}. The same is also the case for the representative frequency of modulation of the meandering motion, which is approximately (1/5) f_{vM}. The low-frequency modulation is statistically in phase on both sides of the wake in each plane, while it is out of phase in the different planes. This indicates that, when the wake is in the phase of enlargement in the major plane, the wake in the minor plane is in the phase of shrinkage, and vice versa. The low-frequency modulation is necessarily of large spatial extent.

The flow field associated with the low-frequency modulation remains to be clarified, together with the mechanism of its origin.

5. Concluding remarks

Vortex structures in the wake of the prototypical three-dimensional bluff bodies have not yet been understood at high Reynolds numbers to the same extent as those in the two-dimensional bluff bodies. This can be demonstrated by the fact that the wake of the circular disk is dominated by helical structures at high Reynolds numbers while no helical structures are observed in the sphere wake, although the linear stability analysis of Natarajan and Acrivos [1] suggests that the unstable modes near the critical Reynolds numbers have the same physical origin in the two bodies.

The base pressure, which is sensitive to changes in vortical structure in the wake [2], is not obtained as a function of Reynolds number even for a sphere. Moreover, the Strouhal number of vortex shedding for the sphere is strongly dependent on Reynolds number. However, only limited information is available on change of flow in the wake associated with the change in the Strouhal number.

The oppositely oriented hairpin vortices in the wake of the elliptic plate are expected to change to the one-sided hairpin vortices in the sphere wake at a critical aspect ratio. The transition may give us further insight into the dynamics of wakes of three-dimensional bluff bodies.

References

[1] R. Natarajan, A. Acrivos, The instability of the steady flow past spheres and disks, J. Fluid Mech. 254 (1993) 323–344.
[2] A. Roshko, Perspectives on bluff body aerodynamics, J. Wind Eng. Ind. Aerodyn. 49 (1993) 101–120.
[3] A.G. Tomboulides, S.A. Orazag, G.E. Karniadakis, Direct and large-eddy simulation of axisymmetric wakes, AIAA Paper 93-0546, 1993.
[4] D. Ormieres, M. Provansal, Transition to turbulence in the wake of a sphere, Phy. Rev. Lett. 83 (1999) 80–83.

[5] R.H. Margarvey, R.L. Bishop, Sphere wakes in liquid systems, Can. J. Phys. 40 (1961) 800–805.
[6] A. Goldburg, B.H. Florsheim, Transition and Strouhal number for the incompressible wake of various bodies, Phys. Fluids 9 (1966) 45–50.
[7] J.S. Wu, G.M. Faeth, Sphere wakes in still surroundings at intermediate Reynolds numbers, AIAA J. 31 (1993) 1448–1455.
[8] H. Sakamoto, H. Haniu, A study on vortex shedding from spheres in a uniform flow, J. Fluids Eng. 112 (1990) 386–392.
[9] R.H. Magarvey, C.S. Maclatchy, Vortices in sphere wakes, Can. J. Phys. 43 (1965) 1649–1656.
[10] T.A. Johnson, V.C. Patel, Flow past a sphere up to a Reynolds number of 300, J. Fluid Mech. 378 (1999) 19–70.
[11] M. Thompson, T. Leweke, M. Provansal, Dynamics of sphere wake transition, J. Fluids Struct. 15 (2001) 575–585.
[12] C. Bouchet, J. Dušek, B. Ghidersa, P. Woehl, Axisymmetry breaking in the wake of a fixed sphere, Book of Abstracts, IUTAM Symposium on Bluff Body Wakes and Vortex-Induced Vibrations, Marseille, France, 2000.
[13] R. Mittal, Planar symmetry in the unsteady wake of a sphere, AIAA J. 37 (1999) 388–390.
[14] H. Sakamoto, H. Haniu, The formation mechanism and shedding frequency of vortices from a sphere in uniform shear flow, J. Fluid Mech. 287 (1995) 151–171.
[15] S. Shirayama, Flow past a sphere: Topological transitions of the vorticity field, AIAA J. 30 (1992) 349–358.
[16] R. Mittal, F.M. Najjar, Vortex dynamics in the sphere wake, AIAA Paper 99-3806, 1999.
[17] H.J. Kim, P.A. Durbin, Observations of the frequencies in a sphere wake and of drag increase by acoustic excitation, Phys. Fluids 31 (1988) 3260–3265.
[18] E. Berger, D. Scholz, M. Schumm, Coherent vortex structures in the wake of a sphere and a circular disk at rest and under forced vibrations, J. Fluids Struct. 4 (1990) 231–257.
[19] K. Kuwahara, Unsteady flow simulation and its visualization, AIAA Paper 99-3405, 1990.
[20] E. Achenbach, Vortex shedding from spheres, J. Fluid Mech. 62 (1974) 209–221.
[21] S. Taneda, Visual observations of the flow past a sphere at Reynolds numbers between 10^4 and 10^6, J. Fluid Mech. 85 (1978) 187–192.
[22] N. Prasad, C.H.K. Williamson, The instability of the shear layer separating from a bluff body, J. Fluid Mech. 333 (1997) 375–402.
[23] S. Cannon, F. Champagne, A. Glezer, Observations of large-scale structures in wakes behind axisymmetric bodies, Exp. Fluids 14 (1993) 447–450.
[24] J.J. Miau, T.S. Leu, T.W. Kiu, J.H. Chou, On vortex shedding behind a circular disk, Exp. Fluids 23 (1997) 225–233.
[25] P.A. Monkewitz, A note on vortex shedding from axisymmetric bluff bodies, J. Fluid Mech. 192 (1988) 561–575.
[26] Y.-H. Kuo, L.V. Baldwin, The formation of elliptic wakes, J. Fluid Mech. 27 (1967) 353–360.
[27] M. Kiya, Y. Abe, Turbulent elliptic wakes, J. Fluids Struct. 13 (1999) 1041–1067.
[28] C. Michalski, L. Schouveiler, M. Provansal, Periodic wakes of spheres and low aspect ratio cylinders, J. Fluids Struct. 15 (2001) 565–573.
[29] C.H. Ho, E. Gutmark, Vortex induction and mass entrainment in a small-aspect-ratio elliptic jet, J. Fluid Mech. 179 (1987) 383–405.
[30] F. Hussain, H.S. Husain, Elliptic jets. Part 1. Characteristics of unexcited and excited jets, J. Fluid Mech. 208 (1989) 257–320.